Available online at www.sciencedirect.com
SCIENCE DIRECT®
Journal of Molecular Graphics and Modelling 24 (2005) 82–93
Journal of Molecular Graphics and Modelling
www.elsevier.com/locate/JMGM

# Direct determination of reaction paths and stationary points on potential of mean force surfaces

Guohui Li, Qiang Cui *

*Department of Chemistry and Theoretical Chemistry Institute, University of Wisconsin, Madison, 1101 University Avenue, Madison, WI 53706, USA*

Accepted 30 May 2005
Available online 7 July 2005

**Abstract**

A simulation approach is introduced for *directly* determining reaction paths and stationary points on potential of mean force (PMF) surfaces associated with molecular events that occur in complex environments. The nudged elastic band approach was employed to search for steepest descent paths on the PMF surface using the relevant PMF derivatives from a series of *local* simulations. The steepest descent path on the PMF surface corresponds to the minimum PMF path (i.e. the path with the lowest local PMF barrier), which contains important information about stationary points (e.g. saddle points) on the PMF surface, which in turn can provide useful insights into the thermodynamics and kinetics for the process of interest. By working with the PMF defined in a low-dimensional subspace rather than a potential energy function of full molecular dimensionality, the main features of the process under study are concisely represented and the *orthogonal* degrees of freedom are adequately sampled with the appropriate canonical distribution at the desired temperature (e.g. 300 K). Therefore, minimum PMF paths carry statistically meaningful mechanistic information and are complementary to reaction paths of full molecular dimensionality proposed in previous studies. The NEB based path optimization method is direct in the sense that no information regarding the *global* PMF surface is necessary for the determination of the *local* reaction path and stationary points along this path. Since only low-dimensional quantities (paths) are searched for, the PMF-path method is expected to scale better in terms of dimension of the PMF subspace than those aims to fully explore multi-dimensional PMF surfaces. Test applications on simple molecular systems, the alanine di-peptide in vacuum and in solution and a microsolvated proton-wire, indicate that reliable PMF paths can be determined for both conformational isomerization and chemical reaction processes. However, highly accurate PMF derivatives are required for determining more quantitative observables, such as the free energy profile along the minimum PMF path. Therefore, effective numerical algorithms for calculating *local* PMF derivatives and systematic protocols for defining the relevant subspace are the main focus in the near future. Finally, we emphasize that the minimum PMF path defined here includes thermal (e.g. entropic) effects associated with the orthogonal degrees of freedom, but finite kinetic energies associated with the PMF degrees of freedom are not included; this can be improved by adopting a different definition of the reaction path, such as the maximum flux path, on the PMF surface, or thermally sampling *all* degrees of freedom orthogonal to the one-dimensional path.


*Keywords:* Simulation; Potential of mean force; Minimum energy path; Nudged elastic band

## 1. Introduction

Since the early simulation studies of Lennard–Jones liquid [1,2], solvated polypeptides [3] and proteins [4], the field of molecular simulation has made impressive progress. Simulations at different length and temporal scales, which are complementary to experimental and theoretical approaches, have become indispensable in the studies of complex systems [5–7]. Among the many remaining challenges, the description of long-time scale processes and rare events is a topic of great significance in many areas of chemistry, biology and physics. Under such a context, the concept of reaction path [8–10] plays an important role. Complementary to detailed dynamical simulations, reaction paths provide a concise description of complex processes, such as chemical reactions in the condensed phase or conformational rearrangements in macromolecules. The reduced representation of reaction paths often makes it easier to perform further analysis, such as the nature of

* Corresponding author.
*E-mail address:* cui@chem.wisc.edu (Q. Cui).

1093-3263/$ – see front matter © 2005 Elsevier Inc. All rights reserved.
doi:10.1016/j.jmgm.2005.06.001

rate-limiting events and factors that make essential contributions. More importantly, the elimination of certain variables makes it computationally more feasible to search for reaction paths than to follow the evolution of the system in full dimensionality. For example, time is not explicitly included in most reaction path based methods, which makes them attractive for describing long-time processes (e.g. protein folding) or rare events (e.g. chemical reaction) that are impossible to follow directly using conventional simulation techniques with standard computational resources.

For small molecular systems in the gas phase, the reaction path of interest is often equivalent or similar to the minimum energy path (MEP) [8,11,12] (or the intrinsic reaction coordinate [10]) on the corresponding *potential energy* surfaces. Due to the relatively small number of degrees of freedom, algorithms for determining reaction paths and stationary points along reaction paths in these systems have been well established [13]. Searching for reaction paths and stationary points on the potential energy surface in the condensed phase is far more challenging for several reasons. Processes that occur in the condensed phase with low rates can be either thermally activated or controlled by spatial diffusions [14,15]. In either case, it is often of interest to include the effect of temperature (e.g. entropic contributions) in the definition of the reaction path, which is not straightforward [16–19]. Moreover, a major challenge from the computational point of view is the high dimensionality [20]. Therefore, although many numerical algorithms can in principle be applied to macromolecules (such as the conjugate peak refinement approach [21] and a family of methods based on replicas [22–24]), the practical complication is that there are a large number of reaction paths with similar energetics or reaction fluxes. Even if the process is dominated by a small number of reaction paths, locating them is not a trivial task if the initial guess is substantially different. In other words, although a handful of paths are often useful for providing qualitative mechanistic insights [25–27], a large number of reaction paths have to be determined to reach more quantitative and robust conclusions. Along this line, the path sampling techniques (TPS) developed by Chandler [28] and others [29] are extremely powerful from the conceptual point of view. The high computational cost, however, makes the application of TPS to macromolecules not yet routinely practical [30]. Moreover, TPS is suited for studying intrinsically fast but rare events, but not designed for studying slow and diffusive processes. For the latter types of problems, the stochastic path approach developed by Elber et al. is promising [31], although convergence of the method in the application to large systems has not been extensively explored.

In the current work, we explored a further reduced description of reaction paths than previous studies with the ultimate aim of developing methods for analyzing the thermodynamics and kinetics of molecular events in complex environments, such as molecular motors. This is motivated by the ever-lasting desire of projecting processes in complex systems into a space of lower dimensionality, and then focus on the behavior of the system in this reduced or coarse-grained space. On the theoretical side, for example, this subspace can be defined by the projector operator scheme that leads to the generalized Langevian equation for the slow variables [32]. From the computational point of view, the subspace can be spanned by a set of variables chosen based on explorative calculations (e.g. using MEP [21,22] or other reaction path methods [18,24]) or physical intuition of the user (see Section 2, for examples). The reduction of the dimensionality makes the search of relevant reaction paths numerically practical for complex systems. We note that the similar subspace-projection idea has been recently adopted by others to explore free energy surfaces with ''meta''- or ''coarse''-molecular dynamics [33–35]; the current work complements those studies in that we focus on determining reaction paths and stationary points (e.g. saddle points) between known reactant and product states. By using a nudged elastic band method, the relevant path and stationary points are determined in a *direct* manner in the sense that no global information regarding the potential of mean force (PMF) surface is needed, in contrast to previous work [36]. The fact a low-dimensional quantity (path) is searched for makes the method particularly useful compared to PMF surface exploration approaches [33,34] when the number of PMF degrees of freedom is large [37]. Although the PMF path requires predetermining a set of essential degrees of freedom to define the PMF (which by itself is perhaps one of the most challenging issues in studying complex processes), the fact that no ad hoc assumption is made *within* the PMF subspace makes the method useful, as far as the PMF subspace contains most important degrees of freedom. In the following, we first describe in details about the definition of our reaction paths and the corresponding computational algorithms for determining such paths in Section 2. Reaction paths in reduced space are illustrated in Section 3 with two simple examples that are related to conformational change problems and chemical reactions, respectively. Finally, we conclude in Section 4 with comments on future developments and applications.

## 2. Methods

### 2.1. Reaction paths on the potential of mean force

As mentioned in Section 1, it is often desirable to establish a low-dimensional subspace that can best describe the process of interest. The spanning coordinates of this subspace can be either local or collective, depending on the particular problem in hand. Although time-scale separation is apparent in certain cases, a meaningful description of many processes in the condensed phase often requires both local and global coordinates. In ion-pair dissociation in

solution, for example, a natural local coordinate is the distance separation between the two ions. As described by previous analysis [38,39], however, it is also crucial to include a set of collective coordinates that represent the effect of solvent reorganization; one possible choice concerns the electrostatic potentials at the two ion sites [33]. Another class of problems where reaction paths of a reduced dimension is useful concerns conformational transitions in macromolecules, such as protein (un)folding processes and functional transitions in molecular motors [40,41]. There the collective coordinates could be the fraction of native contacts [42], radius of gyration [43], which are often used as progressive coordinates in monitoring protein folding [44]. For conformational transitions in biomolecules, meaningful collective coordinates can be defined in terms of low-frequency modes [45–47]. The local variables in these problem could concern the number of water molecules in the core of the protein [48], or pseudo-dihedral angles that define the conformation of essential structural elements in the active site [49]. Although identifying the most important degrees of freedom is an important and challenging subject for studying complex systems, it is not the major focus here; after all, identifying essential degrees of freedom is not the end but rather the beginning of theoretical analysis of complex systems. Our main object is, given a relevant subspace that has been established based on intuition of the researcher or test calculations (e.g. using MEP [21,22] or other reaction path methods [18,24]), to explore the sequence of events during the evolution of the system from the reactant to the product state in this subspace, and to analyze factors that contribute to the corresponding thermodynamics and kinetics.

Denoting the relevant subspace as $\Xi(\mathbf{X})$, and assuming that the rest of degrees of freedom move on a much faster time-scale [50], the *equilibrium* properties of the subspace can then be described in terms of the potential of mean force,

$$W(\Xi,\beta) = -\beta^{-1}\ln\left[\frac{1}{C}\int \mathrm{d}\mathbf{X}\mathrm{e}^{-\beta U(\mathbf{X})}\delta(\Xi'(\mathbf{X})-\Xi)\right] \quad (1)$$

where $\mathbf{X}$ represents all Cartesian degrees of freedom, $\beta$ the inverse temperature and $C$ is the normalization constant (configuration integral). Note that the effect of temperature is rigorously included in the definition of PMF. Due to thermal averaging for the *orthogonal* degrees of freedom, it is often expected that the PMF surface of complex systems is smoother compared to potential energy surfaces [51].

The next step is to define a reaction path that connects the two known stationary states ($R$, $P$) on this PMF surface, $W(\Xi,\beta)$. Similar to previous work in Cartesian space, we can define the reaction path in several ways, depending on the nature of the process. For a diffusive process, for example, one may describe the evolution of the system in the subspace with the Smoluchowski equation [32], and define the reaction path ($l$) as the one with the maximal flux, $j$ (or shortest first passage time, $\tau$) between $R$ and $P$; this corresponds to the MaxFlux path that Huo and Straub [18] proposed based on the original work of Berkowitz et al. [16]

$$\mathrm{Max}\left\{ j_l \propto \frac{1}{\gamma\int_l \exp[\beta W(\Xi)]\,\mathrm{d}l}\right\}$$
$$\sim \mathrm{Min}\left\{\tau_l \propto \frac{1}{D}\int_l \exp[\beta W(\Xi)]\,\mathrm{d}l\right\} \quad (2)$$

where $\gamma$ and $D$ are the friction coefficient and diffusion constant associated with the subspace degrees of freedom (they were assumed to be independent of the degrees of freedom in Eq. (2)). As discussed in a recent study [19], the MaxFlux path can also be expressed in a differential form rather than the integral form in Eq. (2).

Alternatively, one can define the reaction path in a manner similar to the minimum energy path on the potential energy surface, i.e. we define the *minimum PMF path*, which mathematically corresponds to the steepest descent path that connects $R$ and $P$ on the PMF surface,

$$\mathrm{Min}\left\{\int_l W(\Xi)\,\mathrm{d}l\right\} \quad (3a)$$

$$\frac{\mathrm{d}\Xi}{\mathrm{d}l} = -\nabla_\Xi W(\Xi) \quad (3b)$$

The minimum PMF path corresponds to the path with the lowest local PMF barrier height. Physically, this corresponds to the largest rate constant if we assume that the exponential contribution ($\exp(-\Delta W^{\neq})$) overwhelms the effect of pre-factors in either TST or Kramer's rate expressions [14,32]. In this regard, we remind ourselves that the minimum PMF path assumes the adiabatic separation of the $\Xi$ space and the rest degrees of freedom [10,52], and only explicitly includes the thermal effects on the orthogonal degrees of freedom at temperature $1/(k_b\beta)$. The finite kinetic energies associated with the $\Xi$ space can be taken into account when calculating kinetic properties using information of the path (or stationary points along the path) with various rate theories [14]. Nevertheless, since the barrier height is usually the most important component of the rate constant, many previous studies discuss the mechanisms of complex events (e.g. folding of peptides and proteins) in terms of the minimum PMF paths [44,48,53–56].

Compared to previous work that explored paths in full Cartesian space, the PMF paths defined here are in a low-dimensional space, which makes the path *optimization* a more practical task for macromolecules. This is not only because the number of variables needs to be optimized is smaller, but also because the PMF surfaces are in general less rugged compared to potential energy surfaces [51]. The reduction in the number of active variables, however, does not necessarily makes PMF path determination computationally inexpensive because the orthogonal degrees of freedom have to be sufficiently sampled to obtain converged PMF in the relevant subspace; however, as discussed below,

the calculation can be made highly efficient taking advantage of parallel computing. Compared to PMF surface exploration approaches using either fixed or adaptive umbrella sampling [33,35,57–59], the current approach is expected to scale better with dimension of the subspace because a low-dimensional quantity (*path*) rather than an entire multi-dimensional *surface* is sought for. Moreover, since the path is fully *optimized* according to well-defined criterions (Eqs. (2), (3a) and (3b)) within the relevant subspace, the energetics along the path (and other quantities that depend on the energetics, such as rate constants) are more reliable than those from one-dimensional PMF calculations with ad hoc reaction coordinates or approximate reaction coordinates based on the minimum energy path [60].

Finally, we note that as an alternative of the current formulation, one may define the reaction path as the one that minimizes the *one-dimensional* PMF along the path. In other words, instead of exploring a multi-dimensional $W(\Xi(\mathbf{X}))$ as defined by Eq. (1), one explores the one-dimensional PMF in terms of the parameterized path, $l(\mathbf{X})$,

$$W_{1d}(s,\beta) = -\beta^{-1}\ln\left[\frac{1}{C}\int d\mathbf{X} e^{-\beta U(\mathbf{X})}\delta(s'(\mathbf{X}) - s)\right] \quad (4)$$

where $s$ is a variable that characterizes the path length. Accordingly, the minimal PMF path is defined in a similar fashion as Eqs. (3a) and (3b). This formulation assumes the adiabatic decoupling between the path degree of freedom and all the rest, and therefore is more attractive than the multi-dimensional PMF defined in Eq. (1). Due to the parameterization of a general path, calculations of the derivatives of $W_{1d}(s, \beta)$ are less straightforward, although relevant algorithms have been discussed in previous work [60,61]. We were informed recently that developments along this line have been made in the lab of Ren and Vanden-Eijnden as an extension of the string method [62] (Ren and Vanden-Eijnden, private communications).

### 2.2. Searching for the minimum PMF path

In this section, we discuss the numerical algorithm that can be used to determine reactions paths on a low-dimensional PMF surface; in particular, we focus on the minimum PMF path. We emphasize that once a global PMF is available, determining the minimum PMF path numerically is neither difficult nor more informative; with a two-dimensional PMF in hand, for example, one essentially can "eyeball" the minimum PMF path without any calculation. When the dimension of the subspace becomes substantially large [37], however, obtaining a global PMF surface is no longer practical and it is difficult to "eyeball" a favorable reaction path on multi-dimensional surfaces. In those cases, it is highly desirable to have a *direct* method for determining the favorable reaction path without the need of constructing the entire PMF surface, which is the aim of the current development. The solution is based on the consideration that although it is difficult to obtain the *global* PMF surface of a complex system, it is fairly straightforward to compute *PMF derivatives* with respect to the relevant degrees of freedom based on local simulations; in this regard, the problem is rather similar to finding steepest descent paths on the centroid-path-integral surfaces [63], where it is difficult to compute the centroid free energy surface but straightforward to calculate the derivative of the centroid free energy. Therefore, the key is to adopt an algorithm for locating reaction paths that requires *only* the derivative information. Bearing this in mind, we adopted the nudged elastic band (NEB) approach [23], which has been successfully used in MEP determinations for rather complex molecular systems [64].

In the NEB approach, the relevant path is represented by a collection of points with different coordinates, which are often referred to as "images". The minimum PMF path is determined by minimizing the following functional,

$$S^{\mathrm{NEB}}(\Xi_1, \cdots \Xi_{N-1}) = \sum_{i=0}^{N} W(\Xi_i) + \sum_{i=1}^{N}\frac{Nk}{2}(\Xi_i - \Xi_{i-1})^2 \quad (5)$$

where the first term is the descretized expression for the integral of PMF along the path in terms of $N + 1$ "images", and the second term is a penalty term that prevents images from collapsing onto each other. As described previously, an efficient way to determine the NEB path is to use the following modified force of $S^{\mathrm{NEB}}$ with a steepest descent minimization procedure,

$$\mathbf{F}_i^{\mathrm{NEB}} = -\nabla_{\Xi} W(\Xi_i)| + (\mathbf{F}_i^{\mathrm{P}} \cdot \hat{\tau}_{\|})\hat{\tau}_{\|} \quad (6)$$

where the force due to the penalty term in Eq. (5) is given as

$$\mathbf{F}_i^{\mathrm{P}} = Nk_{i+1}(\Xi_{i+1} - \Xi_i) - Nk_i(\Xi_i - \Xi_{i-1}) \quad (7)$$

and $\hat{\tau}_{\|}$ is the unit vector parallel (tangential) to the path [65].

The key quantity in the path optimization process is the determination of the PMF derivatives, $\bigtriangledown_{\Xi}\mathrm{W}$ $(\Xi)$. One straightforward approach is based on constrained MD simulations [66–71],

$$\nabla_{\Xi} W(\Xi_i) = \langle \nabla_{\Xi} U(\mathbf{X}_i) - \beta^{-1}\nabla_{\Xi}\ln|\mathbf{J}|\rangle_{\Xi_i} \quad (8)$$

where the coordinates are honolomically constrained to be specific values associated with the $i$th image. The $U(\mathbf{X}_i)$ is the potential energy function for the $i$th image, and the Jacobian $\mathbf{J}$ appears due to the general non-linear nature of the reaction coordinates, $\Xi$ [67,72]. Although the constrained MD approach has been used extensively for one-dimensional problems [66–68], it is not the most efficient approach for determining PMF derivatives when the dimension of the subspace is higher. This is because one constrained simulation only generates the PMF derivatives for one set of $\Xi$, and information from previous simulations cannot be used once the coordinates for the images are changed during the path optimization. A more attractive

approach is to combine unconstrained MD or efficient MC simulations with adaptive umbrella samplings, such that PMF derivatives for a local region can be obtained and information from many simulations can be effectively combined, e.g. expressions for PMF derivatives from unconstrained simulations have been discussed recently by Darve and Pohorille [71].

Once the minimum PMF path is determined, the energetics along the path (e.g. PMF barrier) can be estimated with a straightforward line-integration,

$$\Delta W^{\neq} = W(\Xi^{\neq}) - W(\Xi_0) = \int_l \mathrm{d}\mathbf{l} \cdot \nabla_{\Xi} W(\Xi) \qquad (9)$$

where the integration is from a stable state (e.g. reactant) to the saddle point on the PMF path. Eq. (8) points to another useful feature associated with the PMF path. It is straightforward to perform component analyses to the energetics, which is valuable for identifying important interactions during the reaction. With the constrained MD approach, for example, this essentially involves computing the components of the potential derivatives ($\bigtriangledown_{\Xi} U$), averaging over the constrained trajectory (Eq. (8)), and finally integrating along the reaction path (Eq. (9)).

Finally, we note that PMF path calculations based on the NEB algorithm can benefit trivially from parallel computations in two major ways. First, different path points (''images'') are independent from each other and, therefore, can be assigned to different nodes. Moreover, for each image, multiple simulations can be carried out in parallel to obtain efficient sampling for the degrees of freedom orthogonal to $\Xi$ and therefore rapid convergence of PMF derivatives with respect to $\Xi$.

## 3. Test calculations

The approach proposed here was tested with two simple examples: the isomerization of the dialanine peptide in vacuum and solution and proton transfers along a proton-wire in a microsolvation environment. These systems were chosen to illustrate that stable results can be obtained for both conformational transition and chemical reaction problems. The low-dimensionality of the chosen subspaces makes it possible to compute the relevant *global* PMF surfaces, which are useful for examining the convergence of minimum PMF path calculations with the NEB algorithm discussed above; we emphasize, here, once again that the PMF path calculations require only local information but not the global PMF surface, in contrast to previous work [36].

The di-peptide was described with the united atom CHARMM force field (Fig. 1a). In the solution simulations, the di-peptide was solvated with a 15.5 Å cubic box of TIP3P water molecules. The proton-wire model (Fig. 1b) was taken from a previous study of Hammes-Schiffer and co-workers [73], where three ''solute'' water molecules plus an extra proton were solvated with a microenvironment consisting of four ''solvent'' water molecules (see Section 3.2 for more details). All the water molecules were treated with an approximate density functional method, SCC-DFTB [74], using the standard set of parameters; these parameters were tested [84] with the standard G2 set of molecules and were shown to give rather encouraging results considering the cost of the calculations.

The subspace for the di-peptide isomerization consists of the familiar backbone dihedral angles, $\phi$ and $\psi$ (Fig. 1a). For the proton-wire problem, the antisymmetric stretch coordinates ($\delta 1$, $\delta 2$; Fig. 1b) associated with the two proton-transfers were chosen. Analytical evaluations of PMF derivatives with the constrained MD approach [37,66,67,75] was tested for the di-alanine peptide in vacuum, which gave very stable results although the Jacobian contribution was not included in the CHARMM implementation. However, constrained MD was not used for other systems because as commented in Section 1, it is not numerically efficient. More robust and proficient approaches for computing analytical PMF derivatives based on unconstrained simulations [70,71] are being pursued. As a convenient scheme to facilitate the minimum PMF path calculations, the PMF derivatives were calculated with a simple finite difference approach in the current work. For each path point, the local region in the relevant subspace is sampled with molecular dynamics and the standard umbrella sampling technique [57]. Multiple simulations with adaptive umbrella potentials (in terms of centers and force constants) were accumulated until a given cut-off is satisfied for the histograms associated with the distribution of subspace variables around the present path point. Data from these simulations were combined with the Weighted Histogram Analysis Method (WHAM) [59] to generate the local PMF, the PMF derivatives were obtained through a bicubic interpolation scheme [76].

In the MD simulations, 1 fs time step was used, and all bonds involving hydrogen were constrained using SHAKE [77]. In the proton-wire simulations, the two transferring protons were not constrained. The temperature of the systems was set to 300 K, which was controlled with Langevian dynamics for the gas phase systems, and with velocity assignment based on Maxwell distributions for the solvated di-peptide.

To establish references for comparison, global potentials of mean force associated with the relevant subspace have also been constructed. For the dialanine, the $\phi - \psi$ PMF was obtained with adaptive umbrella sampling [58]; 6.0 ns of simulations were used for both the vacuum and solution systems, although the vacuum system converged very quickly. For the proton-wire problem, the global PMF as a function of ($\delta 1$, $\delta 2$) was generated with multiple simulations scanning over the relevant space ($\delta_i$ ranges from $-1.0$ to 1.0 Å); 7.2 ns simulations were used. Once the global PMF is available, the relevant minimum PMF path can be determined straightforwardly, which will be regarded as ''exact'' results that can be compared to the minimum PMF

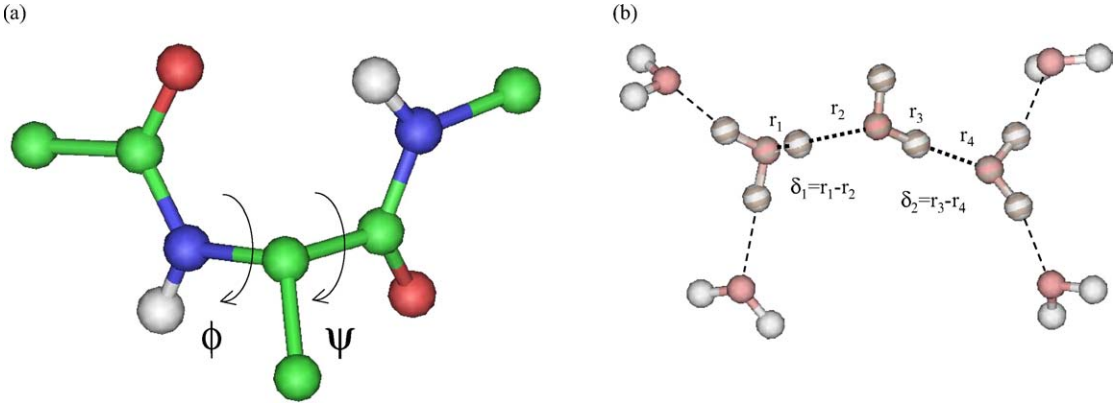


Fig. 1. The two model systems studied for illustrating the PMF paths. (a) The isomerization of the di-alanine peptide, in which the subspace variables are the backbone dihedral angles, $\phi$ and $\psi$. (b) A short proton-wire solvated by four water molecules. The subspace variables are the antisymmetric stretches ($\delta_1$, $\delta_2$) associated with the two sets of proton donor, proton and proton acceptor atoms. The ''solute'' water molecules were under harmonic constraints such that the donor–acceptor distances are close to certain values; the ''solvent'' water molecules were constrained to space with large harmonic constraints on the oxygen atoms (force constant 300 kcal/(mol Å$^{-2}$)).

path determined directly using the NEB algorithms described in Section 2; the latter will be generally referred to as ''NEB path'' in the following discussions. In the NEB calculations, the force constant connecting images was chosen to be 1.0 kcal/(mol Å$^2$); previous experience suggested that NEB results are not very sensitive to the choice of the spring force constant. Path optimizations were stopped when the RMS gradient was below 0.1 kcal/(mol Å).

### 3.1. Alanine di-peptide in the vacuum and in water

In the vacuum case, the minimum PMF path between the $C_{7eq}$ and $C_{ax}$ conformers of the alanine di-peptide was optimized with the NEB approach discussed in Section 2; the two conformers have ($\phi$, $\psi$) values around ($-75^\circ$, $90^\circ$) and ($60^\circ$, $-60^\circ$), respectively. Three initial guesses were used (dashed lines in Fig. 2), which include two rectangular paths (monotonic $\phi$ variation followed by monotonic $\psi$ variation, or vice versa) and one straight-line path. NEB calculations with these three initial guesses led to two distinct minimum PMF paths, which reflects the complexity of the system even in the gas phase. As shown in Fig. 2, with only 12 images, the NEB paths agree very well with the ''exact'' paths determined with the global PMF surface, e.g. both NEB paths pass through the saddle point region.

With the same points in the ($\phi$, $\psi$) space set to be ''reactants ($-75^\circ$, $90^\circ$products ($60^\circ$, $-60^\circ$)'', and the same three sets of initial guesses as in the vacuum case, minimum PMF path calculations were performed for the solvated di-peptide with 12 images. Once again, two distinct paths were found (Fig. 3). Upon solvation, the PMF surface for the alanine di-peptide changed substantially not only the positions of the $C_{7eq}$ and $C_{ax}$ conformers changed significantly, new local minima appeared in the nearby region (Fig. 3). Therefore, each ''exact'' path connecting $C_{7eq}$ and $C_{ax}$ passes through two saddle points and one intermediate state. Encouragingly, the minimum PMF paths optimized with the NEB algorithm successfully captured this feature, and passed through all regions containing critical stationary points (Fig. 3a); the robust nature of the NEB algorithm was reflected by the fact that the path optimizations did not even start from stationary points on the PMF surface. Due to the difficulty associated with accurate PMF derivative calculations in solution (see below), the NEB paths with only 12 images do not match the ''exact'' paths in certain regions, especially where the PMF surface is flat (e.g. where $\phi \sim -100^\circ$, $\psi \sim 20^\circ$). With 30 images, however, we see that the agreement with the NEB paths and ''exact'' results is substantially better (Fig. 3b). In practice, it is efficient to use a small number of images to obtain a coarsely converged minimum PMF path, and then add more images to further refine the results.

To investigate the quantitative aspect of the current computational protocol, we calculated the free energies along the minimum PMF paths according to Eq. (9). The encouraging aspect is that the qualitative trends in free energies were reproduced in both the gas phase and in solution, e.g. the existence of the intermediate state in solution is clearly visible. The quantitative trend, however, is rather disappointing, especially in the solution case (Fig. 4b). Since the NEB paths agree well with the ''exact'' PMF paths, the origin of the errors in relative free energies is the low accuracy of the computed PMF derivatives. As shown in Fig. 5, although there is a good correlation between the PMF derivatives computed on the fly and the ''exact'' results based on the global PMF, large errors were observed quite often. Apparently, the accuracy of the PMF derivatives plays a far more important role in computing relative free energies than determining the minimum PMF path. This is expected because reliable minimum PMF paths can be determined as far as the projection of the PMF derivatives *orthogonal* to the path are small in magnitude, while the relative free energies along the path depend on the precise

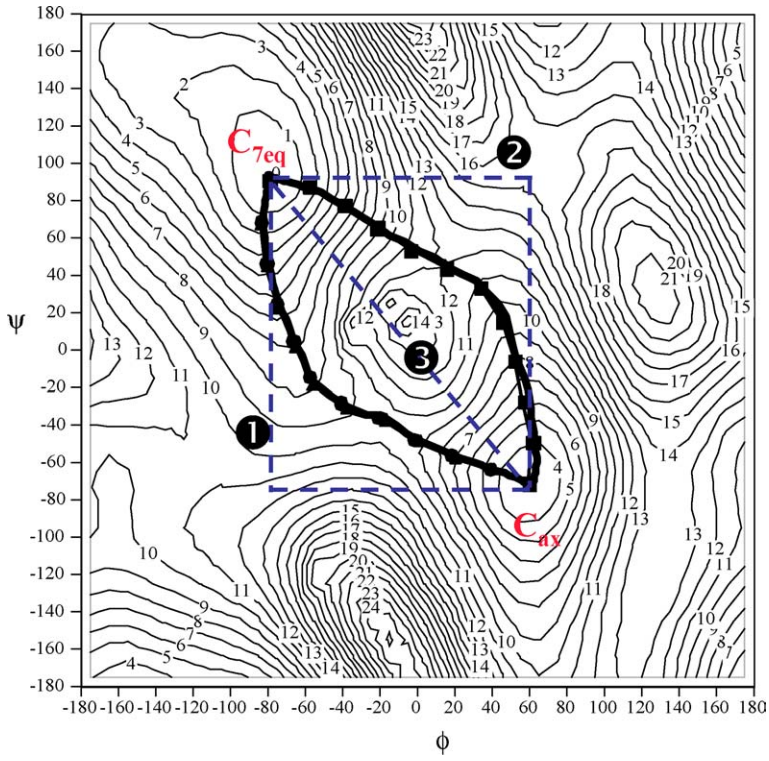


Fig. 2. The global potential of mean force for the di-alanine peptide in vacuum, and PMF paths between $C_{7eq}$ and $C_{ax}$ conformations at 300 K. Three initial guesses (dotted lines) were used in the nudged elastic band (NEB) based PMF path optimizations, which led to two distinct PMF paths; the three sets of converged results are indicated with different symbols (diamond, circles and triangles). The bold solid lines are the "exact" paths obtained based on finite-difference derivatives of the global PMF surface. Clearly, the NEB paths agree well with the "exact" paths with only 12 images.

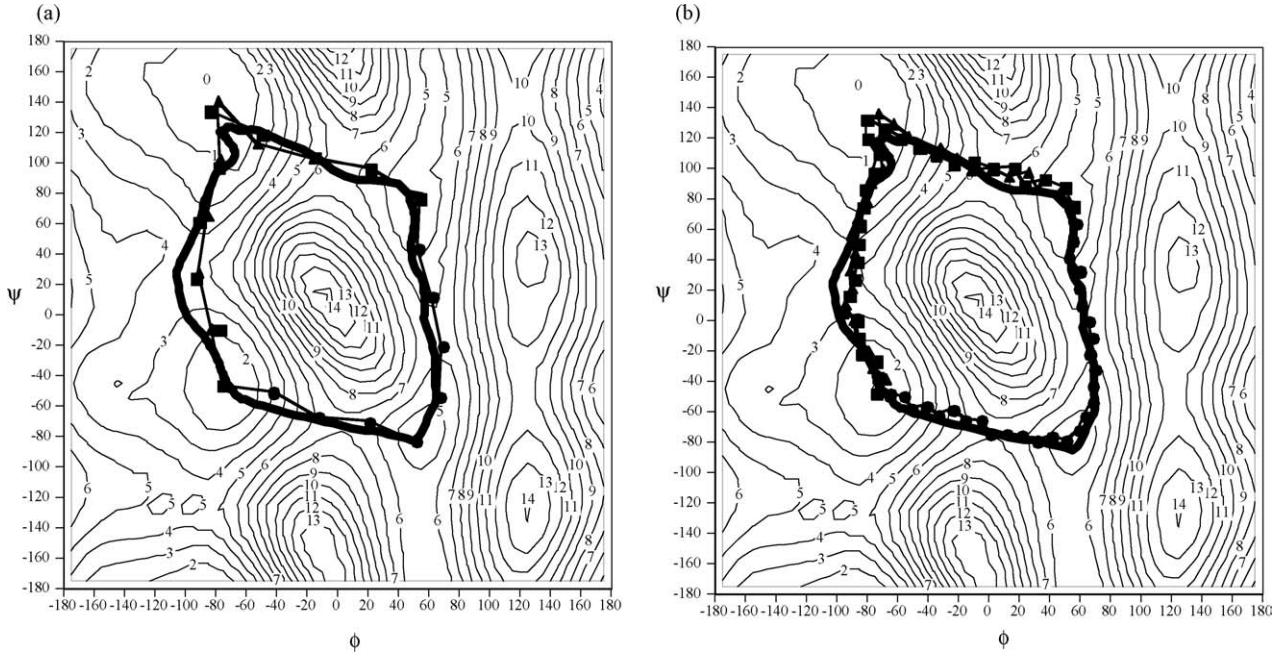


Fig. 3. Similar to Fig. 2 but for the solvated di-alanine peptide. The same three sets of initial guesses as in Fig. 2 was used. In (a) and (b), 12 and 30 images were used, respectively. The bold solid lines are the "exact" paths obtained based on finite-difference derivatives of the global PMF surface.

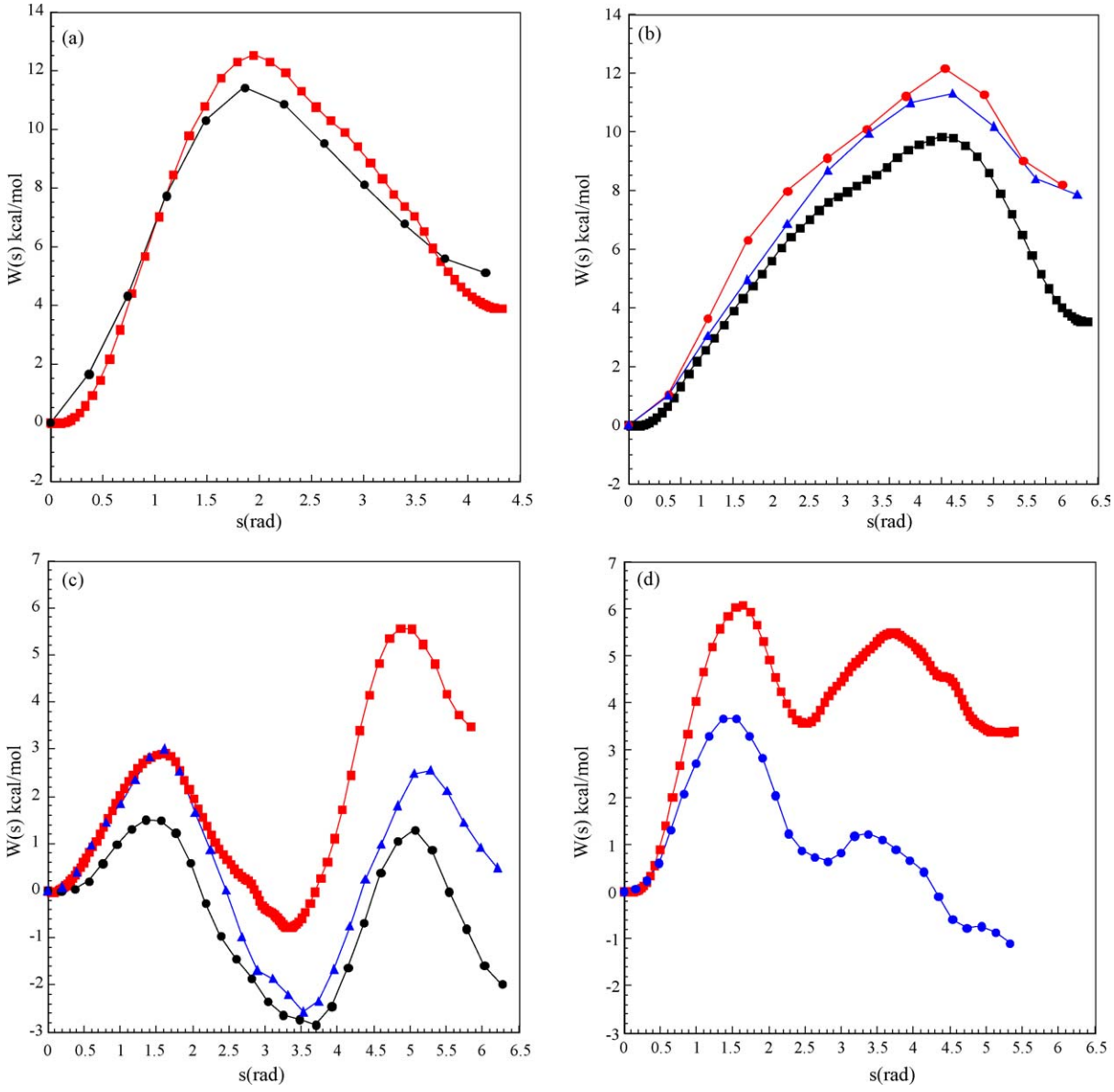


Fig. 4. Relative free energies along the PMF path based on line integration of the PMF derivatives (Eq. (8)). (a) Path 1 for di-alanine in vacuum; (b) path 2 and 3 for di-alanine in vacuum; (c) path 1 and 3 for di-alanine in water and (d) path 2 for di-alanine in water. The lines with many points are results from ''exact'' paths, while others are from NEB calculations. Clearly, the qualitative trends are reproduced well by NEB calculations; the quantitative aspects, however, remain to be improved with better simulation protocols for the PMF derivatives.

value of the PMF derivatives projected *onto* the path. Therefore, to make the minimum PMF path approach quantitatively useful, the next challenge is to develop computational protocols that deliver accurate PMF derivatives [70,71].

### *3.2. Proton transfers along a micro-solvated proton-wire*

Long-range proton transfers play an important role in many chemical and biological systems [78,79]. One of the relevant mechanistic questions is whether the protons transfer in a concerted or step-wise (i.e. with kinetically distinct intermediate) manner, and how environment might modulate the transfer mechanism. Previous model studies by Hammes-Schiffer and co-workers [73] have clearly demonstrated that the coupling between multiple proton transfers is sensitive to the nearby solvent configurations and relative positions of the proton donor and acceptor atoms. It was found that proton transfers tend to be strongly coupled when a long donor–accepter distance is followed by a short one (e.g. 3.0 and 2.8 Å, respectively) because it is not energetically favorable to have an extra proton in the middle when the donor–acceptor distance is long. Although such non-equilibrium studies are very powerful in illustrating factors that influence proton transfer mechanisms, identifying the dominant mechanism requires averaging real-time simulations over a large number of starting configurations.

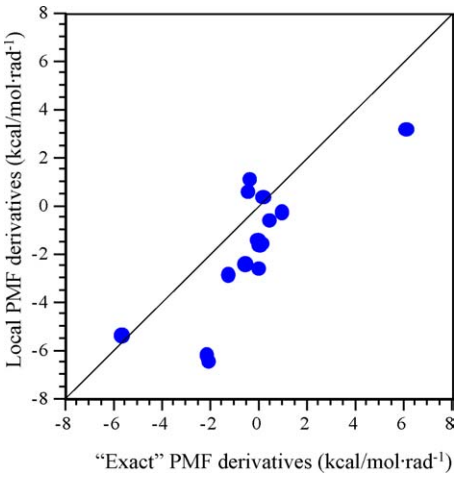


Fig. 5. Correlation between the PMF derivatives calculated on-the-fly based on local simulations and "exact" results based on finite-difference of the global PMF surface for randomly selected points on the $\phi$, $\psi$ map for a solvated di-alanine peptide. A modest correlation ($R^2 = 0.62$) was found. Clearly, the quality of the PMF paths (Fig. 3) is less sensitive to the accuracy of the PMF derivatives compared to the relative free energies along the paths (Fig. 4).

Here, we take the alternative equilibrium approach, and characterize the dominant mechanism by minimum PMF paths.

The proton-wire model (Fig. 1b) is the same as the one constructed by Hammes-Schiffer and co-workers [73], which contains three water molecules plus an extra proton, and four water molecules that represent the micro-solvent environment. The solute water molecules were constrained with harmonic potentials on the donor–acceptor distances; this is necessary because otherwise the extra proton tends to localize at the middle water in the cluster model. Two cases were investigated, where the donor–acceptor distances are restrained to be close to 2.8–2.8 and 3.0–2.8 Å, respectively, with harmonic potentials (force constant ~100 kcal/(mol Å$^{-2}$)). The two cases were motivated by the previous observation [73] mentioned above that proton transfers appear to be strongly coupled if a long donor–acceptor distance is followed by a short one; we want to explore if this trend holds based on the corresponding PMF surfaces and whether minimum PMF path calculations are useful for providing mechanistic insights in this regard. The solvent molecules were constrained in space with a harmonic force constant of 300 kcal/(mol Å$^2$) to prevent them from evaporating from the solute at 300 K.

Before discussing the minimum PMF paths, we first comment on the global PMF surfaces associated with the two model cases. Both cases involve an intermediate in which the first proton transfer has finished and the second one is yet to occur, i.e. the proton transfers appear to be stepwise. However, we note that when the two donor–acceptor distances are asymmetrical, the barrier for the second proton transfer is very low, on the order of 1 kcal/mol. Therefore, kinetically speaking, the second proton transfer is likely to be strongly coupled to the first proton transfer, as found in the previous dynamics study of Hammes-Schiffer and co-workers. We also note that the present calculations do not include nuclear quantum effects, which might further increase the concerted nature of the proton transfers.

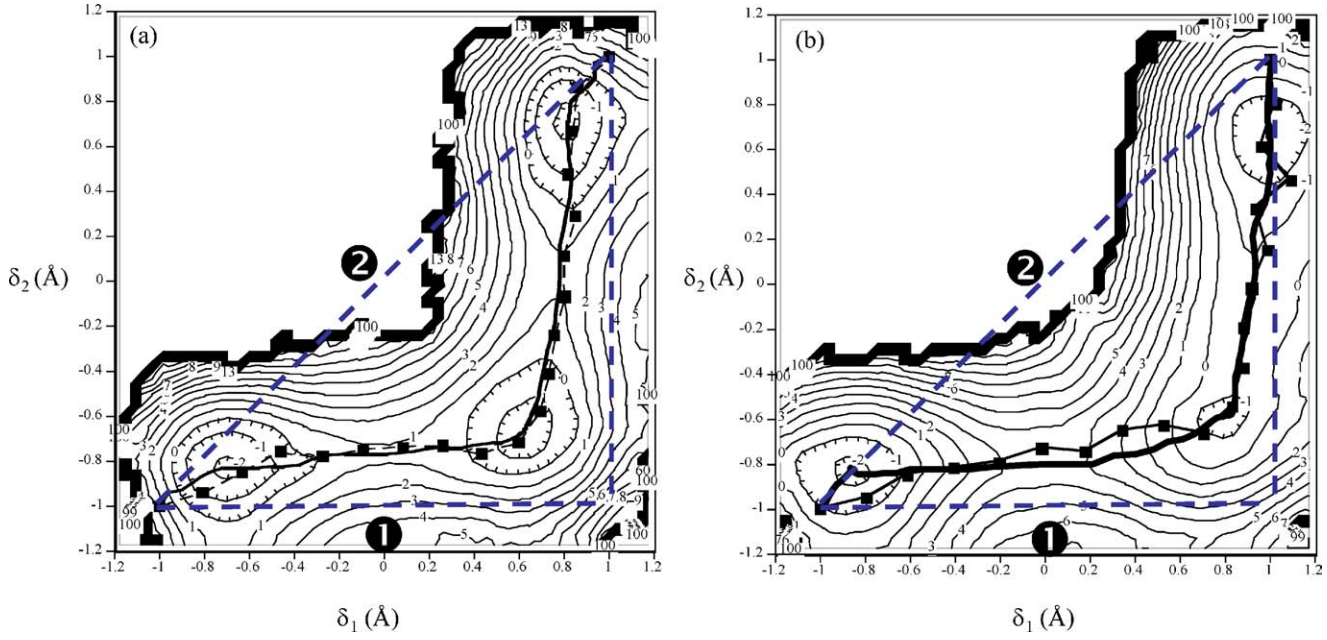


Fig. 6. The global potential of mean force for a short proton-wire solvated by four water molecules (Fig. 1b and PMF paths associated with the proton transfers at 300 K. In (a) the two sets of donor–acceptor atoms were restrained to be close to 2.8 Å and 2.8 Å, respectively; in (b) they were restrained to be close to 3.0 Å and 2.8 Å, respectively. Two initial guesses (dotted lines) were used in the nudged elastic band (NEB) based PMF path optimizations, which led to essentially the same path; therefore, only one set of result was shown for each case. The bold solid lines are the "exact" paths obtained based on finite-difference derivatives of the global PMF surface. Clearly, the NEB paths agree well with the "exact" paths with only 20 images except for regions where the PMF is flat.

However, the purpose of the present study is to illustrate minimum PMF path calculations for chemical reactions, thus no attempts have been made to correct for the missing nuclear quantum effect, which can be included with centroid path-integral simulation [80] for the PMF derivatives.

As to the minimum PMF paths, the NEB calculations with 20 images gave rather smooth paths that are close to the ''exact'' steepest descent paths on the PMF surface. These calculations indicate that, for both sets of models, proton transfers proceed in a step-wise manner, i.e. significant variations in $\delta 1$ and $\delta 2$ take place in different segments of the paths (Fig. 6). In the case where the two sets of donor–acceptor distances are restrained to be close to 3.0 and 2.8 Å, respectively, the PMF in the product region is flat, which led to some zig–zag behavior of the NEB path (Fig. 6b). The kinetic coupling between the two sets of proton transfers is not evident based on the path alone, and free energies along the path are crucial for any mechanistic insights. The latter relies on, however, that the PMF derivatives are sufficiently accurate. Similar to the di-peptide situation, the PMF derivatives calculated with the current protocol are adequate for optimizing reliable minimum PMF paths, but they are not quantitatively reliable for computing free energies along the path (not shown). Once again, this emphasizes the importance of developing efficient algorithms for computing reliable PMF derivatives. Alternatively, once a reliable minimum PMF path has been located with PMF derivatives of mediocre accuracy, one can parameterize the path and then perform separate *one-dimensional* PMF calculations using the more conventional umbrella sampling technique [57,59].

## 4. Concluding remarks

A new computational technique for characterizing the mechanism of molecular processes that occur in complex environments has been explored; encouraging results have been obtained for two simple test systems: isomerization of dialanine and multiple proton transfers in microsolvated proton-wires. The basic idea is to *directly* explore reaction paths (e.g. minimum PMF paths) and stationary points on potential of mean force surfaces without any global information regarding this surface; although it is easy to ''eyeball'' favorable reaction paths once a global PMF surface is available for low-dimensioanl problems, a systematic and *direct* method is crucial for problems that require many degrees of freedoms to define the PMF subspace. Because reaction path approaches in general do not explicitly contain temporal information, they are ideal for exploring the mechanism of rare-events and long-time-scale processes, such as chemical reactions in the condensed phase and conformational transitions in macromolecules, respectively. By working with the potential of mean force rather than potential energy, a low-dimensional subspace is chosen to concisely represent the main features of the process under study, and the orthogonal degrees of freedom are adequately sampled with the appropriate canonical distribution at the desired temperature (e.g. at 300 K). As a result, the minimum PMF paths are easier to search for from an optimization point of view, and they carry statistically meaningful mechanistic information. Although the PMF degrees of freedom are assumed to be adiabatically decoupled from the rest in the minimum PMF path, the effect of finite temperature on the PMF subspace can be taken into account with various rate (e.g. Kramers') theories in kinetics studies. Therefore, the minimum PMF path and the stationary points along this path can provide useful thermodynamic and kinetic information regarding the process of interest. In short, the PMF-path approach proposed here is complementary to previous reaction path [9,17–19,22,24] and dynamical path methods [28,29,33] that are based on full dimensionality representation of complex systems. Compared to other coarse-grained approaches designed for exploring PMF surfaces [33–35], the current approach should scale better in terms of the dimension of the PMF subspace because a low-dimensional quantity (path) rather than a higher-dimensional surface is sought for; for realistic applications, however, one might have to optimize multiple paths for robust results (see below).

The key elements to meaningful PMF path calculations include the choice of relevant variables and sufficient sampling of the orthogonal degrees of freedom. Although the two simple test systems used local geometrical coordinates, such as the $\phi$, $\psi$ dihedral angles in peptides and antisymmetric stretch coordinates in proton-wires, it is conceivable that additional collective coordinates are useful for condensed phase systems. Good examples for the latter include electrostatic field at the reaction site, fraction of native contacts and low-frequency normal coordinates, which are useful for describing chemical reactions in solution, folding of peptides and proteins and conformational transitions in molecular motors, respectively. With the combination of appropriate collective and local coordinates, PMF path searches are expected to be useful for exploring mechanisms of complex molecular events. The practical limitation is that although local coordinates are easy to identify, it is less straightforward to pick the most relevant collective coordinates, which have to come from chemical/physical intuitions of researchers or explorative simulations (e.g. using MEP [21,22] or other reaction path methods [18,24]).

Given a set of subspace variables, we optimize the minimum PMF path using an algorithm based on the nudged elastic band approach, which was originally proposed for optimizing reaction paths on potential energy surfaces [23]. The advantage of the NEB approach is that it requires only the first order derivatives, and it does not require highly accurate information about the stationary points along the path. Instead of using potential energy derivatives, the derivatives of the PMF are required in minimum PMF path optimizations, which were calculated using constrained MD

simulations or a finite-difference approach coupled to *local* umbrella sampling in the current work. Test calculations with simple models (alanine di-peptide in vacuum and in solution, and microsolvated proton-wire) indicated that the calculated PMF derivatives are sufficient for determining well-behaved PMF paths; for more quantitative results such as relative free energies along the minimum PMF path, the demand on the accuracy of PMF derivatives is substantially higher. Therefore, a major challenge for the near future is to develop numerically efficient and accurate ways to compute PMF derivatives.

Finally, we note that the NEB approach we used is a local optimization protocol, thus the resulting path depends on the initial guess, as evident already in simple systems as the di-alanine peptide. To find the dominant path, if it exists, multiple calculations with different initial guesses are required. With the reduced dimensionality and roughness associated with PMF surfaces compared to full-dimensional potential energy surfaces, however, the problem is expected to be substantially less severe. Moreover, we have focused on classical potential of mean force surfaces, which may not be adequate for problems that exhibit significant nuclear quantum effects, such as multiple proton transfers in macromolecules [27,81–83]. In those cases, the average contribution from nuclear quantum effects can be included in the PMF calculations with centroid path-integral methods [63,80].

## Acknowledgements

We thank Prof. Kuczera for discussions concerning PMF derivative calculations. This work was partially supported by the starting-up fund from the Department of Chemistry and College of Letters and Science at University of Wisconsin, Madison, and a Research Innovation Award from the Research Corporation. Q.C. is an Alfred P. Sloan Fellow.

## References

[1] A. Rahman, MD simulation of LJ liquid, Phys. Rev. 136A (1964) 405.
[2] B.J. Berne, J. Jortner, R. Gordon, Vibrational relaxation of diatomic molecules in gas and liquids, J. Chem. Phys. 47 (1967) 1600.
[3] P.J. Rossky, M. Karplus, Solvation. A molecular dynamics study of a dipeptide in water, J. Am. Chem. Soc. 101 (1979) 1913–1937.
[4] J.A. McCammon, B.R. Gelin, M. Karplus, Dynamics of folded proteins, Nature 267 (1977) 585–590.
[5] J. Berne, G. Ciccotti, D.F. Coker, Classical and Quantum Dynamics in Condensed Phase Simulations, World Scientific, Singapore, 1998.
[6] S.D. Schwartz, Progress on Theoretical Chemistry and Physics, Kluwer Academic, Dordrecht, 2000.
[7] M. Karplus, J.A. McCammon, Molecular dynamics simulations of biomolecules, Nat. Struct. Biol. 9 (2002) 646–652.
[8] D. Heidrich, The Reaction Path in Chemistry: Current Approaches and Perspectives, Kluwer, Dordrecht, 1995.
[9] R. Elber, Reaction path studies of biological molecules, in: R. Elber (Ed.), Recent Developments in Theoretical Studies of Proteins, World Scientific, New York, 1996.
[10] K. Fukui, The path of chemical reactions—the IRC approach, Acc. Chem. Res. 14 (1981) 363–368.
[11] R.A. Marcus, Analytical mechanics of chemical reactions, III. Natural collision coordinates, J. Chem. Phys. 49 (1968) 2610–2616.
[12] D.G. Truhlar, Potential Energy Surfaces and Dynamics Calculations, Plenum Press, New York, 1981.
[13] H.B. Schlegel, Optimization of equilibrium geometries and transition structures, Adv. Chem. Phys. 67 (1987) 249.
[14] P. Hanggi, P. Talkner, M. Borkovec, Reaction-rate theory: fifty years after Kramers, Rev. Mod. Phys. 62 (1990) 251–341.
[15] M. Karplus, Aspects of protein reaction dynamics: deviation from simple behavior, J. Phys. Chem. 104 (2000) 11–27.
[16] M. Berkowitz, et al. J. Chem. Phys. 79 (1983) 5563.
[17] R. Elber, D. Shalloway, Temperature dependent reaction coordinates, J. Chem. Phys. 112 (2000) 5539–5545.
[18] S. Huo, J.E. Straub, MaxFlux, J. Chem. Phys. 107 (1997) 5000.
[19] R. Crehuet, M.J. Field, A temperature-dependent nudged-elastic-band algorithm, J. Chem. Phys. 118 (2003) 9563–9571.
[20] H. Frauenfelder, S.G. Sligar, P.G. Wolynes, The energy landscape and motions of proteins, Science 254 (1991) 1598–1603.
[21] S. Fischer, M. Karplus, Conjugate peak refinement: an algorithm for finding reaction paths and accurate transition state in systems with many degrees of freedom, Chem. Phys. Lett. 194 (1992) 252–261.
[22] R. Elber, M. Karplus, A method for determining reaction paths in large molecule: application to myoglobin, Chem. Phys. Lett. 139 (1987) 375–380.
[23] G. Henkelman, B.P. Uberuaga, H. Jonsson, A climbing image nudged elastic band method for finding saddle points and minimum energy paths, J. Chem. Phys. 113 (2000) 9901–9904.
[24] R. Olender, R. Elber, Calculation of classical trajectories with a very large time step: formalism and numerical examples, J. Chem. Phys. 105 (1996) 9299–9315.
[25] A. Ghosh, R. Elber, H. Scherage, An atomically detailed study of the folding pathways of protein A with the stochastic difference equation, Proc. Natl. Acad. Sci. U.S.A. 99 (2002) 10394–10398.
[26] S. Huo, J.E. Straub, Proteins: structure, function and genetics, Proteins 36 (1999) 249s.
[27] Q. Cui, M. Karplus, Quantum mechanics/molecular mechanics studies of triosephosphate isomerase-catalyzed reactions: effect of geometry and tunneling on proton transfer rate constants, J. Am. Chem. Soc. 124 (2002) 3093–3124.
[28] P.G. Bolhuis, et al. Transition path sampling: throwing ropes over rough mountain passes, in the dark, Annu. Rev. Phys. Chem. 53 (2002) 291–318.
[29] D. Parsserone, M. Ceccarelli, M. Parrinello, A concerted variational strategy for investigating rare events, J. Chem. Phys. 118 (2003) 2025–2032.
[30] P.G. Bolhuis, C. Dellago, D. Chandler, Reaction coordinates of biomolecular isomerization, Proc. Natl. Acad. Sci. U.S.A. 97 (2000) 5877–5882.
[31] R. Elber, et al. Bridging the gas between long time trajectories and reaction pathways, Adv. Chem. Phys. 126 (2003) 93.
[32] R. Zwanzig, Nonequilibrium Statistical Mechanics, Oxford University Press, Oxford, 2001.
[33] A. Laio, M. Parrinello, Escaping free energy minima, Proc. Natl. Acad. Sci. U.S.A. 99 (2002) 12562–12566.
[34] G. Hummer, I.G. Kevrekidis, Coarse molecular dynamics of a peptide fragment: free energies, kinetics, and long-time dynamics computations, J. Chem. Phys. 118 (2003) 10762–10773.
[35] M. Iannuzzi, A. Laio, M. Parrinello, Efficient exploration of reactive potential energy surfaces using car-parrinello molecular dynamics, Phys. Rev. Lett. 90 (2003) 238302.
[36] J. Apostolakis, P. Ferrara, A. Caflisch, Calculation of conformational transitions and barriers in solvated systems: application to the alanine dipeptide in water, J. Chem. Phys. 110 (1999) 2099–2108.

[37] J. Mahadevan, K.-H. Lee, K. Kuczera, Conformational free energy surfaces of Ala10 and Aib10 peptide helices in solution, J. Phys. Chem. B 105 (2001) 1863–1876.
[38] P.L. Geissler, C. Dellago, D. Chandler, Kinetic pathway of ion pair dissociation in water, J. Phys. Chem. B 103 (1999) 3706–3710.
[39] D.G. Truhlar, B.C. Garrett, Multidimensional transition state theory and the validity of Grote-Hynes theory, J. Phys. Chem. B 104 (2000) 1069–1072.
[40] K.C. Holmes, M.A. Geeves, Structural mechanism of muscle contraction, Annu. Rev. Biochem. 68 (1999) 687–728.
[41] F. Julicher, A. Ajdari, J. Prost, Modeling molecular motors, Rev. Mod. Phys. 69 (1997) 1269–1281.
[42] A.R. Dinner, et al. Understanding protein folding via free-energy surfaces from theory and experiment, TiBS 25 (2000) 331–339.
[43] E.M. Boczko, C.L. Brooks III, First-principles calculation of the folding free energy of a 3-helix bundle protein, Science 269 (1995) 393–396.
[44] J.E. Shea, C.L. Brooks III, From folding theories to folding proteins: a review and assessment of simulation studies of protein folding and unfolding, Annu. Rev. Phys. Chem. 52 (2001) 499–535.
[45] G. Li, Q. Cui, Analysis of functional motions in "Brownian molecular machines" with an efficient block normal mode approach. myosin-II and $Ca^{2+}$-ATPase, Biophys. J. 86 (2004) 743–763.
[46] Y.A. Berlin, et al. Conformationally gated rate processes in biological macromolecules, J. Phys. Chem. A 105 (2001) 5666–5678.
[47] G. Basu, et al. A collective motion description of the 3-10/alpha-helix transition—implications for a natural reaction coordinate, J. Am. Chem. Soc. 116 (1994) 6307–6315.
[48] J.E. Shea, J.N. Onuchic, C.L. Brooks III, Probing the folding free energy landscape of the src-SH3 protein domain, Proc. Natl. Acad. Sci. U.S.A. 99 (2002) 16064–16068.
[49] P. Roche, et al. Molecular dynamics of the FixJ receiver domain: movement of the beta 4-alpha 4 loop correlates with the in and out flip of Phe101, Protein Sci. 11 (2002) 2622–2630.
[50] A.M. Berezhkovskii, et al. Reaction dynamics on a thermally fluctuating potential, J. Chem. Phys. 111 (1999) 9952–9957.
[51] J.N. Onuchic, P.G. Wolynes, Energy landscapes, glass transitions, and chemical-reaction dynamics in biomolecular or solvent environment, J. Chem. Phys. 98 (1993) 2218–2224.
[52] R. Olender, R. Elber, J. Mol. Struct. Theochem. 398–399 (1997) 63–72.
[53] T. Lazaridis, et al. Reaction paths and free energy profile for conformational transitions: AN internal coordinate approach, J. Chem. Phys. 95 (1991) 7612–7625.
[54] J.J. Portman, S. Takada, P.G. Wolynes, Microscopic theory of protein folding rates. I. Fine structure of the free energy profile and folding routes from a variational approach, J. Chem. Phys. 114 (2001) 5069–5081.
[55] J.J. Portman, S. Takada, P.G. Wolynes, Microscopic theory of protein folding rates. II. Local reaction coordinates and chain dynamics, J. Chem. Phys. 114 (2001) 5082–5096.
[56] N.D. Socci, J.N. Onuchic, P.G. Wolynes, Diffusive dynamics of the reaction coordinate for protein folding funnels, J. Chem. Phys. 104 (1996) 5860–5868.
[57] G.M. Torrie, J.P. Valleau, Non-physical sampling distributions in Monte Carlo free energy estimation: umbrella sampling, J. Comp. Phys. 23 (1977) 187–199.
[58] C. Bartels, M. Karplus, Probability distributions for complex systems: adaptive umbrella sampling of the potential energy, J. Phys. Chem. B 102 (1998) 865–880.
[59] S. Kumar, et al. The weighted histogram analysis method for free energy calculations on biomolecules. 1. The method, J. Comput. Chem. 13 (1992) 1011–1021.
[60] E. Neria, S. Fischer, M. Karplus, Simulation of activation free energies in molecular systems, J. Chem. Phys. 105 (1996) 1902–1921.
[61] R. Elber, Calculation of the potential of mean force using molecular dynamics with linear constraints: an application to a conformational transition in a solvated dipeptide, J. Chem. Phys. 93 (1990) 4312–4321.
[62] E.W.W. Ren, E. Vanden-Eijnden, Phys. Rev. B 66 (2002) 052301.
[63] Y. Brumer, et al. Calculating approximate quantum mechanical rates without an a priori reaction coordinate, J. Chem. Phys. 116 (2002) 8376–8383.
[64] H. Jonsson, Theoretical studies of atomic-scale processes relevant to crystal growth, Annu. Rev. Phys. Chem. 51 (2000) 623–653.
[65] G. Henkelman, H. Jonsson, Improved tangent estimate in the nudged elastic band method for finding minimum energy paths and saddle points, J. Chem. Phys. 113 (2000) 9978–9985.
[66] E.A. Carter, G. Ciccotti, J.T. Hynes, Constrained reaction coordinate dynamics for the simulation of rare events, Chem. Phys. Lett. 156 (1989) 472–477.
[67] M. Sprik, G. Ciccotti, Free energy from constrained molecular dynamics, J. Chem. Phys. 109 (1998) 7737–7744.
[68] T. Mulders, et al. Free energy as the potential of mean constraint force, J. Chem. Phys. 104 (1996) 4869–4870.
[69] J. Schlitter, M. Klahn, A new concise expression for the free energy of a reaction coordinate, J. Chem. Phys. 118 (2003) 2057–2060.
[70] W.K. den Otter, W.J. Briels, The calculation of free-energy differences by constrained molecular dynamics simulations, J. Chem. Phys. 109 (1998) 4139–4146.
[71] E. Darve, A. Pohorille, Calculating free energies using average force, J. Chem. Phys. 115 (2001) 9169–9183.
[72] M. Fixman, Classical statistical mechanics of constraints: A theorem and application to polymers, Proc. Natl. Acad. Sci. U.S.A. 71 (1974) 3050–3053.
[73] H. Decornez, K. Drukker, S. Hammes-Schiffer, Solvation and hydrogen-bonding effects on proton wires, J. Phys. Chem. 103 (1999) 2891–2898.
[74] M. Elstner, et al. Self-consistent-charge density-functional tight-binding method for simulations of complex materials properties, Phys. Rev. B58 (1998) 7260–7268.
[75] Y. Wang, K. Kuczera, Exploration of conformational free energy surfaces of helical Ala and Aib peptides, J. Phys. Chem. B 101 (1997) 5205–5213.
[76] W. Press, et al. Numerical Recipes in Fortran 77, second ed., Cambridge University Press, Cambridge, 1996.
[77] J.P. Ryckaert, G. Ciccotti, H.J. Berendsen, Numerical integration of the cartesian equations of motion of a system with constraints: molecular dynamics of *n*-alkanes, J. Comp. Phys. 23 (1977) 327–341.
[78] R.A. Copeland, S.I. Chan, Proton translocation in proteins, Annu. Rev. Phys. Chem. 40 (1989) 671–698.
[79] M. Wikstrom, Proton translocation by bacteriorhodopsin and heme-copper oxidases, Curr. Opin. Struct. Biol. 8 (1998) 480–488.
[80] G.A. Voth, Path-integral centroid methods in quantum statistical mechanics and dynamics, Adv. Chem. Phys. XCIII (1996) 135–218.
[81] S.R. Billeter, et al. Hydride transfer in liver Alcohol dehydrogenase: quantum dynamics, kinetic isotope effects, and role of enzyme motion, J. Am. Chem. Soc. 123 (2001) 11262–11272.
[82] J. Gao, D.G. Truhlar, Quantum mechanical methods for enzyme kinetics, Annu. Rev. Phys. Chem. 53 (2002) 467–505.
[83] R. Pomes, B. Roux, Free energy profiles for H+ conduction along hydrogen-bonded chains of water molecules, Biophys. J. 75 (1998) 33–40.
[84] T. Kruger, M. Elstner, P. Schiffels, T. Frauenheim, Validation of the density function based tight-binding approximation method for the calculation of reaction energies and other data, J. Chem. Phys. 122 (2005), Art. 114110.